Biochimica et Biophysica Acta, 1064 (1991) 111–123

ADONIS 0005273691001753

BBAMEM 75168

A mathematical model of rabbit cortical thick ascending limb of the Henle's loop

P.L. Fernandes and H.G. Ferreira

Laboratory of Physiology, Department of Cell Biology, Gulbenkian Institute of Science, Oeiras (Portugal)

(Received 2 June 1990)

Key words: Henle's loop; Mathematical model; (Rabbit kidney)

A mathematical version of the cell model of the cortical thick ascending limb of the rabbit proposed by Greger and Schlatter ((1983) Pflügers Arch. 396, 325–334) is described. Available data are sufficient to compute the most important parameters. Simulations of experiments with perfused tubules in which the transepithelial voltage and conductance, and the intracellular electrical potential were measured in the course of ionic substitutions in the perfusing baths or treatment with ouabain or furosemide are in good agreement with the experimental results with the exception of those relating to dilution potential experiments. The model can be used in the analysis and planning of experiments and is capable of predicting the instantaneous values of ionic fluxes and intracellular concentrations and of cell volume.

Introduction

As a result of recent progress in the characterization of the functional properties of the rabbit thick ascending limb (cTAL) [1], Greger and Schlatter [2] were able to propose a cell model based on linear circuit analysis which predicts most of the published results obtained under steady state conditions. The present work is an attempt to produce a mathematical version of that cell model, along the lines proposed by Lew et al. [3], and to test its capability to predict both the steady state and the transient behaviour of the preparation. Using this approach we are able to compute the transient values of the most commonly observable variables (transepithelial conductance, electrical potential differences and fractional resistances across the apical and basolateral barriers). The model provides also the instantaneous values of other variables such as intracellular concentrations and fluxes of the different ions, but at this stage we shall concern ourselves only with the question of whether it predicts adequately the published experimental observations. The model is interactive and can be run on a personal computer of modest performance.

Correspondence: H.G. Ferreira, Laboratory of Physiology, Department of Cell Biology, Gulbenkian Institute of Science, Oeiras, Portugal.

Methods

Our mathematical model is entirely based on that proposed by Greger and Schlatter [2] and is depicted in Fig. 1. It corresponds to a single-layer epithelium across which there are movements (diffusional or mediated) of Na^+, K^+ and Cl^-. The system is driven by a Na^+/K^+ pump and, under open-circuit conditions, performs a net transport of NaCl from the luminal to the basolateral compartment. There is no net transport of K^+ across the cells but there is a small diffusional, paracellular, net transport of this ion towards the basolateral

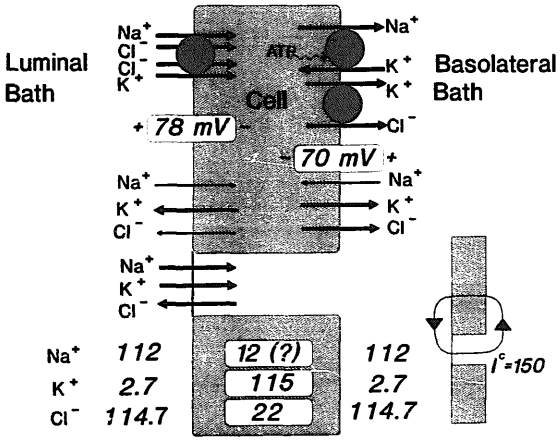

Fig. 1. The cell model.

side. Fluxes represented by thin lines in Fig. 1 are negligible when compared to the other fluxes. Under steady-state and open-circuit conditions two Cl^- ions per Na^+ cross the cells. This generates a positive circulating current I^c which flows through the cells towards the luminal side and through the paracellular pathway in the opposite direction.

The numerical model

The model presented in this paper is based on a number of assumptions.

1. Geometry

The cTAL will be treated as a flat sheet of 1 cm^2 area and 1.5 μm thickness. The simulations correspond to experiments performed at high perfusion rates while constancy of composition of the lumen and peritubular baths was maintained. Under such conditions the open circuit transepithelial potential will be uniform along the tube as it is assumed to be uniform over the whole area of the the modelled epithelial sheet.

2. The bathing fluids

The bathing fluids are assumed to contain only sodium, potassium and chloride. This assumption does not pose serious constraints since the rabbit cTAL transports bicarbonate, protons, amino acids, glucose or phosphates at negligible rates [1]. In the simulated ion substitution experiments sodium, potassium or chloride or any combination of them were replaced isotonically. As in Greger [1] ion activities will be used in the computations, tables and graphs, throughout the paper.

3. The cell compartment and the movements of water

The cell compartment is assumed to contain only sodium, potassium, chloride and nondiffusible anions of an average valence n. The activity and valence of the nondiffusible ions are initially adjusted so as to obtain isotonicity and electroneutrality in the cell compartment. The total amount and valence of intracellular nondiffusible ions is assumed to be constant at all times. We have also assumed that the movements of water across the cell membranes are so rapid in comparison with those of the ions that isotonicity is kept by instantaneous changes in cell volume. No water movements across the whole epithelium are considered, since the rabbit cTAL is not a volume transporter, and since, under the conditions simulated here, there is no osmotic gradient across the epithelium.

4. Transepithelial ionic movements

The transport mechanisms encoded in the model are those proposed by Greger and Schlatter [2] and are depicted in Fig. 1. A Na-K-2Cl cotransport with the affinities for sodium, potassium and chloride proposed by Greger and co-workers [1] is placed in the luminal membrane, and a Na^+/K^+ pump together with a low-affinity K-Cl cotransport are placed in the basolateral membrane. The rate of transport mediated by the K-Cl cotransporter is encoded by adjusting the phenomenological coefficient $(A^{bl})_{cot}$ (see List of symbols, p. 121) in such a way that it corresponds to a fraction, β, between 0 and 1, of the potassium flux through the Na^+/K^+ pump. The value of β determines also the size of the diffusional fluxes of potassium across the basolateral barrier hence, the diffusional potassium permeability of the same barrier. The diffusional movements of sodium, potassium and chloride across the two cell membranes and through the paracellular pathway are assumed to obey the Goldman-Hodgkin-Katz (GHK) equation [5]. The permeabilities of the apical membrane to sodium and chloride and the permeability of the basolateral membrane to sodium, although very small (0.1 $nm\,s^{-1}$), are included in the model to allow the possibility of changing their magnitudes should the need for that arise. The permeability of the luminal membrane to potassium is initially adjusted so that the net flux of potassium across that membrane is zero under control conditions. It can, however, be changed in order to obtain a net transepithelial transport of potassium. The permeability of the basolateral membrane to chloride is initially adjusted so as to give no net cell accumulation or loss of chloride under control conditions. Potassium, sodium and chloride are assumed to diffuse through the paracellular route according to the GHK equation and the corresponding permeabilities (P_K^{sh}, P_{Na}^{sh} and P_{Cl}^{sh}) obey the ratios 3 : 2.5 : 1 [1].

5. Conservation relationships

The model is constrained by three conservation relationships:

(a) Isotonicity. See Section 3 above.

(b) Mass conservation is encoded on the assumption that the rate of accumulation of an ion in the cell compartment at any instant is given by the difference between its influx across the luminal membrane and its outflux across the basolateral membrane.

(c) Electroneutrality is implicit in the application of Kirchoff's laws to the model. The total current across the luminal membrane is always equal to the total current flowing across the basolateral membrane and the total transepithelial current is at any time equal to the sum of the transcellular current with the paracellular current. In addition the total charge due to the

positive ions is equal to that due to the negative ions in the three compartments.

The set of equations

(a) Kinetic equations

1. Diffusional currents

Diffusional currents are given by the GHK equation of the general form

$$I_i = \frac{Z_i \cdot F \cdot E}{[\exp(E)-1]} \cdot [C_i^1 \cdot \exp(E) - C_i^2]$$

where I_i is the current density ($A\,cm^2\,s^{-1}$) of ion i across a given barrier, Z_i (equiv. mol^{-1}) is the valence of ion i and C_i^1, C_i^2 ($mol\,cm^{-3}$) are the activities of ion i on sides 1 and 2 of the barrier. In this model side 1 corresponds to the mucosal or to the cell comparments and side 2 to the cell or to the basolateral compartments. E (dimensionless) is given by the expression

$$E = Z_i \cdot F \cdot V / R \cdot T$$

where F is the Faraday constant (96 500 coul equiv.$^{-1}$), V is the electrical potential difference (volt) across the barrier, R is the gas constant (8.314 $J\,mol^{-1}\,K^{-1}$) and T the absolute temperature (K).

2. Specialized transport systems

(a) Sodium pump. The sodium ($(F_{Na})_p$) and potassium ($(F_K)_p$) pump fluxes are given by

$$(F_{Na})_p = (F_{Max})_p \cdot \left(\frac{C_{Na}^c}{C_{Na}^c + K_{Na}}\right)^3 \cdot \left(\frac{C_K^{bl}}{C_K^{bl} + K_k}\right)^2$$

$$(F_K)_p = -(2/3) \cdot (F_{Na})_p$$

where C_{Na}^c is the activity of sodium in the cell compartment and C_K^{bl} is the activity of potassium in the basolateral bath. K_{Na} (2.6 mM) and K_K (0.56 mM) are the apparent affinities of the pump for sodium (cell compartment side) and potassium (basolateral side), respectively, and their values were taken from Lew et al. [3].

(b) Na-K-2Cl symport. This cotransport system was encoded as

$$(F^1)_{cot} = (F_{Max})_{cot} \cdot \left\{ \frac{C_{Na}^l}{C_{Na}^l + (K_{Na})_{cot}} \cdot \frac{C_K^l}{C_K^l + (K_K)_{cot}} \cdot \frac{(C_{Cl}^l)^2}{(C_{Cl}^l)^2 + [(K_{Cl})_{cot}]^2} - \frac{C_{Na}^c}{C_{Na}^c + (K_{Na})_{cot}} \cdot \frac{C_K^c}{C_K^c + (K_K)_{cot}} \cdot \frac{(C_{Cl}^c)^2}{(C_{Cl}^c)^2 + [(K_{Cl})_{cot}]^2} \right\}$$

$$(F^l)_{cot} = (F_K^l)_{cot} = (F_{Na}^l)_{cot} = (1/2) \cdot (F_{Cl}^l)_{cot}$$

where in general $(F_i^l)_{cot}$ is the flux of ion i (Na, K or Cl) through the symport located in the luminal membrane, C_i^l and C_i^c are the activities of ion i in the lumen (l) and cell (c) compartments, respectively and $(K_i)_{cot}$ is the affinity for ion i of the symport. $(F_{Max})_{cot}$ is the transport rate at complete saturation. The chosen affinity constants for the three ions were: $(K_{Na})_{cot} = 2.5$ mM; $(K_K)_{cot} = 1.5$ mM; $(K_{Cl})_{cot} = 55$ mM [1].

(c) K-Cl symport. Since there is no information available about the affinity for potassium and chloride of this system we use the simplest kinetic discription.

$$(F^{bl})_{cot} = (A^{bl})_{cot} \cdot (C_K^c \cdot C_{Cl}^c - C_K^{bl} \cdot C_{Cl}^{bl})$$

where $(A^{bl})_{cot}$ is a phenomenological constant ($mol^{-1}\,cm^4\,s^{-1}$), and, in general, C_i^c and C_i^{bl}, where i may be Cl or K, are the activities of ion i in the cell (c) and basolateral compartments (bl). $(F^{bl})_{cot}$ is the flux of K or Cl across the K-Cl symport located in basolateral membrane.

3. Electroneutrality

Electroneutrality is encoded by the following relationships.

$$C_{Na}^c + C_K^c = C_{Cl}^c + n \cdot C_{An}^c$$

where C_{An}^c is the intracellular activity of nondiffusional ions (An) of valence n. Similar equations are written for the external compartments but containing terms only for Na, K and Cl.

$$I^l = I^{bl}$$

$$I^l + I^{sh} = I^{bl} + I^{sh} = I_{tot}$$

where I^l, I^{bl}, I^{sh} and I_{tot} are the total currents flowing at any instant across the luminal membrane, the basolateral membrane, the paracellular pathway and the whole epithelium, respectively.

4. Isotonicity

Isotonicity is expressed in the relationship

$$C_{Na}^c + C_K^c + C_{Cl}^c + C_{An}^c = C_{iso}$$

where C_{iso} is the osmolarity of the bathing fluids under control conditions.

5. Conservation of mass

Conservation of mass is ensured by the following differential equations:

$$dQ_{Na}/dt = \Sigma F^{l}_{Na} - \Sigma F^{bl}_{Na}$$

$$dQ_{K}/dt = \Sigma F^{l}_{K} - \Sigma F^{bl}_{K}$$

$$dQ_{Cl}/dt = \Sigma F^{l}_{Cl} - \Sigma F^{bl}_{Cl}$$

where, in general, F_i^l and F_i^{bl} (i may be Na, K or Cl) are the fluxes of ion i across the luminal and the basolateral membranes, respectively, and Q_i (mol cm^{-2}) is the total amount of ion i in one cm^2 of epithelium.

Computing strategy

Borrowing the terminology from the economists [6] the model deals with three types of quantities: parameters (diffusional permeabilities, affinities and maximal rates of transport through the specialized transport systems and the total amount and valence of nondiffusible ions); exogenous variables (ion activities in the bathing fluids and the transepithelial current); endogenous variables (transepithelial potential, the electrical potential across the two cell membranes, the intracellular ion activities and the cell volume).

The system of equations is first solved for a steady state situation (reference state) so as to obtain a self-consistent set of values for the parameters.

After the steady state is defined, experimental situations can be simulated by relaxing one or more exogenous variables (ion substitution experiments, or experiments of current injection) or by changing one or more parameters (to simulate the effects of transport inhibitors). To simulate the effects of ouabain and and furosemide $(F_{Max})_p$ and $(F_{Max})_{cot}$ were reduced to 1% of their corresponding reference values. Similar reductions in P_K^l and P_K^{bl} were introduced in the simulation of the barium experiments. This is probably an overestimate of the barium effect but in the absence of quantitative measurements of this effect the choice of any other value is equally arbitrary. The model computes the time course of the endogenous variables by integrating the differential equations which describe the rates of change of the ion content of the cells and by computing the instantaneous volume of the cell compartment. In some simulations the steady state was computed directly [7].

The conductances calculated by the model are slope conductances obtained by differentiating the GHK equation in relation to voltage. The values thus obtained are identical to those computed by simulating experiments in which a small current pulse is injected across the preparation.

Fitting of the numerical model to the experimental data

Ideally the numerical model should be fitted to the experimental data by relaxing the derived parameters through a minimizing algorithm. We did not attempt such technique because, for obvious reasons, papers in which sufficient number of variables were measured in the same tube are not available. This means that the average values given by Greger [1] may not, and most likely do not, apply to any individual tube. Such situation, which is the rule with epithelia, defeats any attempt at using an automatic minimizing technique since there is no unique and self-consistent set of experimental values. The strategy adopted in this work follows very closely that described by Lew et al. [3]. We started with a set of values of the observable intensive variables (activities of sodium, potassium and chloride in the luminal, cell and basolateral compartments and electrical potential differences across the apical and the basolateral membranes) and we postulated a value of 150 μA cm^{-2} for the circulating current I^c as suggested by Greger [1]. We were left with four undetermined parameters: the diffusional permeabilities of the apical barrier to sodium and chloride, the diffusional permeability of the basolateral barrier to sodium and β. We could have introduced the conductances of the apical and the basolateral barriers as two additional constraints but, since a large number of other experimental values had to be fitted, we chose instead to define a minimal version of the model (reduced model) in which $\beta = 0.75$ and $P_{Cl}^l = P_K^l = P_{Na}^l = 0.1$ nm cm^{-1}. In the course of the simulations we relaxed individually each of these parameters in an attempt to select the most satisfactory set of values. To completely define the reference state a few aditional assumptions had to be encoded. Namely, the kinetics of the K-Cl cotransport, the kinetics of the sodium pump and the assumption that the diffusional movements of the ions across the three barriers (luminal, basolateral and paracellular) are adequately described by GHK equation. With these assumptions and with the set of input variables listed above, the system is well placed and can be completely solved for the steady state.

Results

A. The reference state

When the average values of the observable quantities given in Greger [1] are used as inputs, the model computes the parameters marked with * reported in Table I thus completing the definition of the reference state. Table I also shows that the conductances of the luminal and basolateral barriers (8.4 and 9.2 mS cm^{-2}, respectively) are lower than the average experimental values (12 and 30 mS cm^{-2}, respectively) reported by Greger

TABLE I

Reference state

Symbols: l, luminal barrier or compartment; bl, basolateral barrier or compartment; c, cell compartment; sh, shunt pathway; tot, transepithelial; I_c, circulating current in $\mu A cm^{-2}$. Activities in mM; permeabilities in $nm cm^{-1}$; voltages in mV; conductances in $mS cm^{-2}$. Values signaled with * are outputs of the model; all the other values were input to the model. $I_c = 150$.

	l	c	bl	sh	tot
Na^+	112	12	112		
K^+	2.7	115	2.7		
Cl^-	114.7	22	114.7		
P_{Na}	0.1		0.1	313 *	
P_K	1440 *		195 *	376 *	
P_{Cl}	0.1		618 *	138 *	
V	78		−70		8
G	8.4		9.2 *	18.8 *	23

[1]. In Figs. 2A and 2B we analysed the sensitivity of these variables to one of the parameters (β) and to four of the variables (I^c, C^c_K, C^c_{Cl} and V^l). For very low input values of P^l_{Cl} and P^l_{Na} (see Table I) the conductance of the luminal barrier (G^l) is determined by P^l_K which will be larger the larger the circulating current (I^c) and the smaller the electrochemical gradient for potassium across this barrier, hence the high sensitivity of G^l to C^c_K and V^l. G^{bl} on the other hand is mainly due to the high permeability of the basolateral barrier to chloride (see Table I) and this permeability is determined by the input values of the circulating current and by the electrochemical gradient for chloride across the basolateral barrier. A steep dependence of G^{bl} in relation to C^c_{Cl} and V^l is observed when this activity approaches its equilibrium value. However, adjustments in V^l (hence in V^{bl}) have opposite effects on G^l and G^{bl}. G^{bl} can also be increased by reducing the input value of β which entails an increase in P^{bl}_K. Proper manipulation of these five input quantities will improve the matching between experimental and computed values of G^{bl} and G^l. The same can be achieved by manipulating P^{bl}_{Na}, P^l_{Cl} and P^l_{Na} (Figs. 2C and 2D). As a result of the high values of P^l_K, P^{bl}_K and P^{bl}_{Cl} these permeabilities will still be dominant if the input values of P^{bl}_{Na}, P^l_{Cl} and P^l_{Na} are increased up to three orders of magnitude. A final choice between these different alternatives can only be made by imposing additional constraints obtained from more experimental data.

B. Steady-state response to changes in the ion composition of the bathing fluids

The overall design of these experiments consists of recording the response of some of the endogenous variables to step changes in the ionic composition of the bathing fluids after the transient of the responses is over.

In most of the published experiments on the cTAL the endogenous variables recorded are: transepithelial conductances and voltages; intracellular electrical potential; voltage divider ratios (VDR). To compare the

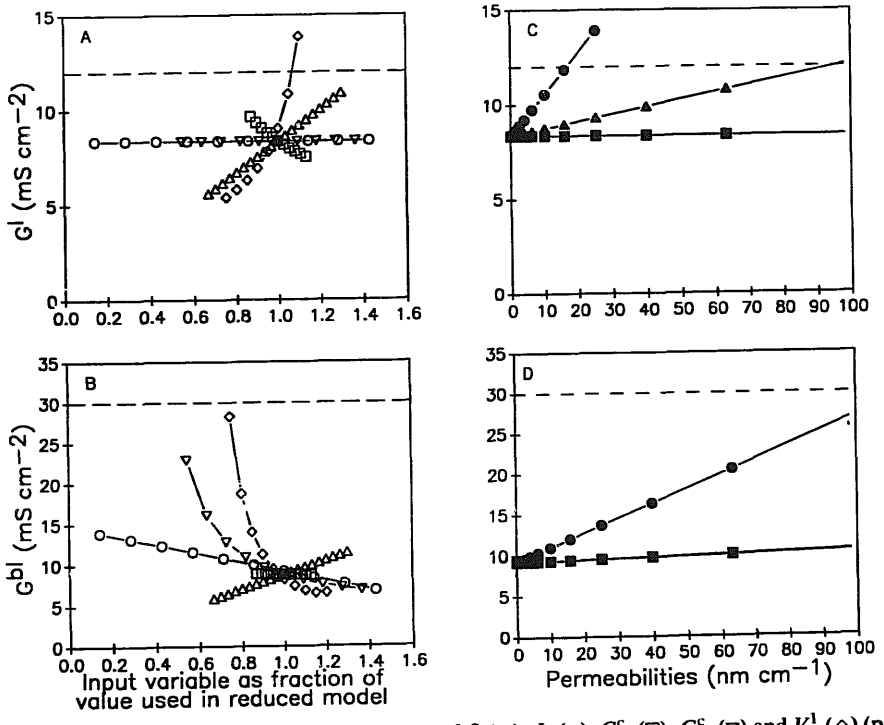

Fig. 2. Sensitivity of G^l and G^{bl} of the reference state to the input values of β (○), I_c (△), C^c_K (□), C^c_{Cl} (▽) and V^l (◇) (panels A and B) and of P^l_{Na} (●), P^l_{Cl} (▲) and P^{bl}_{Na} (■) (Panels C and D). Only one input variable or parameter was stepped at a time. All the other were given the corresponding values reported in Table I. Dashed lines: experimental values of G^l and G^{bl} as given in Greger [1].

simulations with published experiments, the model, as depicted in Table I, is used as one of the reference states (reduced model). To see if changes in the reference state lead to improvements in the fitting of the computed responses to the experimental curves, a number of changes in the input variables, one at a time, were introduced. The simulations involved thus two steps. First, the reference state was obtained, and then the response to the perturbation in one or more exogenous variables or parameters (effect of barium) was computed. The simulations presented below are just a small fraction of those possible and aim at providing hints of how individual input variables or parameters can influence the response of the model. To reduce the number of simulations we have chosen to change the four unconstrained parameters (P^{bl}_{Na}, P^{l}_{Cl}, P^{l}_{Na} and β) by one order of magnitude per step but we do not report simulations which are very far away from the experimental findings. As a result of the way in which the model is constructed a reduction in the value of β entails a compensating increase in P^{bl}_{K} (hence in the potassium conductance of the basolateral barrier) so that the potassium flux balance across the basolateral barrier is maintained.

1. Properties of the luminal membrane [8]

Table II reports the steady-state responses to activity steps of potassium and chloride and to the addition of barium (99% reduction in P^{l}_{K}) on the luminal side represented by the differences between the values measured or computed at steady state after the perturbation and those corresponding to the reference state. In relation to V^{l}, computed and measured values do not differ by more than 22.5%. In particular, it should be noticed that reduction of chloride on the luminal side causes an hyperpolarization as observed experimentally, instead of the depolarization to be expected from a purely diffusional process. It is not easy to compare the values of V_{tot} because in the original paper values of this variable are only given for typical experiments and because the transepithelial voltage is always very small in the cTAL (less than 10 mV). Furthermore, in ion substitution experiments, V_{tot} can be strongly influenced by spurious diffusion potentials of the same order of magnitude, whose value may be estimated only approximately. There is also some uncertainty as to the experimental value of VDR [9]. The only large discrepancy between computed and experimental values arises in the reduced model in relation to the change in VDR induced by barium (760 versus an experimental value of 34) and may be due to several factors; barium may have a smaller effect on P^{l}_{K} than that used in the simulation; the values of P^{l}_{Na} and/or P^{l}_{Cl} may be larger than those used in the reduced model. In both cases the residual G^{l} after adding barium would be larger with a consequent decrease in ΔVDR. With this exception, the simulations reported in Table II are not very sensitive to the values of P^{l}_{Na} or P^{l}_{Cl}.

2. Properties of the basolateral membrane [2]

Published data on the response of the intracellular electrical potential to ion susbtitutions on the basolateral bath display a large scatter. Increasing C^{bl}_{K} from 2.7 to 13.9 mmoll^{-1} may have no effect on V^{bl} or may depolarize it by up to 35 mV. However, most of the depolarizations are in the range of 10 to 25 mV. The reduced model yelds a value of 6.7 mV (Table III). This is because with $\beta = 0.75$, P^{bl}_{Cl} dominates the permeabil-

TABLE II

Simulations of experiments in which (first column): C^{l}_{K} was raised to 13.9 mM, or C^{l}_{Cl} reduced to 34.4 mM or P^{l}_{K} reduced to 1% of its reference value (effect of barium)

For each of these experimental situations three reference states (second column) were used corresponding to: the reduced model (see Table I); to a reference state with a P^{l}_{Na} of 100 nmcm^{-1}; to a reference state with a P^{l}_{Cl} of 100 nmcm^{-1}. The simulations involved first the solution of the reference state for each of the three cases of column 2 and then the computation of the response to the perturbation in C^{l}_{K}, C^{l}_{Cl} or P^{l}_{K} untill a steady state was reached. Experimental values were obtained from Ref. 8. Computed (columns 3, 4 and 5) and experimental values (columns 6, 7 and 8) tabled correspond to the differences between those computed or measured at steady state after the perturbation and the corresponding reference or control values. For units see Table I.

Experimental condition	Model	Computed values			Experimental values		
		ΔV_{tot}	ΔV^{l}	ΔVDR	ΔV_{tot}	ΔV^{l}	ΔVDR
$C^{l}_{K}=13.9$	Reduced	−3.3	24.6	−0.38	−2	20.4	0.2
	$P^{l}_{Na}=100$	−6.1	23.0	−0.32			
	$P^{l}_{Cl}=100$	−6.7	25.0	−0.28			
$0.01\times P^{l}_{K}$	Reduced	−5.0	26.4	760	−2	22	34
	$P^{l}_{Na}=100$	−12.4	28.7	13.1			
	$P^{l}_{Cl}=100$	−5.7	27.6	8.8			
$C^{l}_{Cl}=34.4$	Reduced	−7.0	−13.0	0.85		−7.0	
	$P^{l}_{Na}=100$	−9.9	−7.8	0.74			
	$P^{l}_{Cl}=100$	−13.8	−7.7	0.73			

TABLE III

Simulations of experiments in which (first column): C_K^{bl} was raised to 13.9 mM, or C_{Cl}^{bl} reduced to 34.4 mM or P_K^{bl} or P_K^{bl} and $(F^{bl})_{cot}$ reduced to 1% of their reference values (effect of barium)

For each of these experimental situations four reference states (second and third columns) were used corresponding to: the reduced model (see Table I) with $\beta = 0.75$ or $\beta = 0.01$; to a reference state with a P_{Na}^{bl} of 100 nmcm^{-1} and $\beta = 0.75$ or 0.01. For the chloride experiments a fixed value of β (0.75) was used because the results do not depend on β. The simulations involved first the solution of the reference state for each of the three cases of columns 2 and 3 and then the computation of the response to the perturbation in C_K^l, C_{Cl}^l or P_K^l untill a steady state was reached. Experimental values were obtained from Ref. 2. Computed (columns 4, 5 and 6) and experimental values (columns 7, 8, 9) tabled correspond to the differences between those computed or measured at steady state after the perturbation and the corresponding reference or control values. For units see Table I.

Experimental condition	Model	Computed values			Experimental values		
		ΔV_{tot}	ΔV^{bl}	ΔVDR	ΔV_{tot}	ΔV^{bl}	ΔVDR
$C_K^{bl} = 13.9$	Reduced	2.0	−6.7	−0.3	(?)	(−4 to −35)	(?)
	$\beta = 0.01$	3.0	−11.0	0.27			
$P_{Na}^{bl} = 100$	$\beta = 0.75$	2.8	−10.8	0.12			
	$\beta = 0.01$	4.27	−16.2	0.61			
$0.01 \times P_K^{bl}$	Reduced	0.58	−3.15	−0.18	(?)	(0 to −65)	0
	$\beta = 0.01$	1.96	−10.1	−0.56			
$P_{Na}^{bl} = 100$	$\beta = 0.75$	1.47	−7.61	−0.61			
	$\beta = 0.01$	4.5	−21.5	−1.82			
$0.01 \times P_K^{bl}$ and	Reduced	1.6	−8.2	−0.091			
$0.01 \times (F^{bl})_{cot}$	$\beta = 0.01$	1.98	−10.2	−0.53			
$P_{Na}^{bl} = 100$	$\beta = 0.75$	3.25	−16	−0.56			
	$\beta = 0.01$	4.5	−21.6	−1.81			
$C_{Cl}^{bl} = 34.4$	Reduced	−7.14	−12.5	2.05	4(?)	(−8 to −60)	(?)
$P_{Na}^{bl} = 100$		−6.3	−7.8	1.47			

ity of the basolateral barrier (see Table I). If P_K^{bl} is increased either by reducing β and/or by increasing P_{Na}^{bl} (hence the rate of pumping and recirculation of potassium across the basolateral barrier) the computed depolarization can go up to 16 mV. Experimentally the effect of barium from the basolateral side on V^{bl} is a depolarization ranging from a negligible value to 60 mV. The barium effect was simulated in two ways; a reduction of P_K^{bl} by 99% and a reduction of both P_K^{bl} and $(F^{bl})_{cot}$ (see List of symbols) by the same amount. Depolarizations up to 21 mV could be obtained in the last case. In the experiments in which C_{Cl}^{bl} in the basolateral bath was reduced to 1/3 of the control value two types of responses were observed: small transient depolarizations of around 8 mV and large depolarizations up to 60 mV. In our simulations we obtained steady depolarizations of 12.5 mV in the reduced model and 7.8 mV when P_{Na}^{bl} was increased to 100 nmcm^{-1}. The smaller increase in the last case resulting from the relative loss of selectivity to chloride of the basolateral barrier due to a larger value of P_K^{bl}. On the whole the values obtained with the simulations are within the range of the experimental findings but as a result of the variability of the experimental data we cannot use them to constrain the values of β or P_{Na}^{bl} any further.

3. Ionic selectivity of the whole epithelium [9]

The cation selectivity of the cTAL has been studied by measuring the response of the transepithelial electrical potential to ionic gradients. This response should depend on the behaviour of the two cell barriers (luminal and basolateral) and also on the ionic selectivity of the paracellular pathway and since the conductance of this pathway accounts for at least 70% of the total transepithelial conductance [1] it should dominate the overall response of the preparation. At the present stage a detailed simulation of diffusional potentials caused by gradients to ions other than those considered in the reduced model seems unwarranted since it would entail the introduction of additional flux equations which cannot be based on flux measurements. Instead, we chose the simplest experimental situation in which NaCl is isotonically substituted on the luminal or the basolateral baths by an inpermeant non-dissociable molecule (mannitol). Fig. 3 depicts the results of the computations together with the experimental results. Simulations with the reduced model do not give a good fit to the experimental data. The response to a reduction in NaCl on the basolateral compartment is rather flat as a result of the high permeability of the basolateral barrier to chloride. As expected the fitting is not improved by

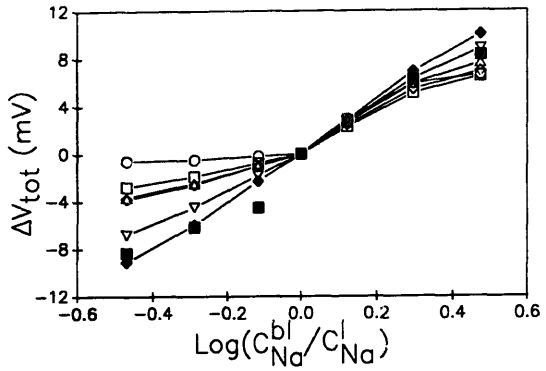

Fig. 3. NaCl dilution potentials across the whole epithelium. NaCl replaced isotonically on either side. V_{tot} in mV. Permeability values in $nmcm^{-1}$. Values plotted correspond to the published experimental curve (■) and to simulations in which five models were used; reduced (△, see Table I); $P^{l}_{Na} = 100$ (○); $P^{l}_{Cl} = 100$ (□); $P^{bl}_{Na} = 100$ (◆); $\beta = 0.01$ (◇); $V_{tot} = 4$ mV (▽). For meaning of symbols see List of symbols.

changes in P^{l}_{Cl}, P^{l}_{Na} or β but is very reasonable when P^{bl}_{Na} is increased or when the overall permeability of the parallel pathway is increased by reducing the transepithelial potential from 8 to 4 mV.

4. Sodium dependence of the equivalent short-circuit current [10]

The sodium dependence of the equivalent I_{sc} was studied experimentally by measuring V_{tot} and G_{tot} at different activities of sodium on both sides of the preparation using choline as a replacement ion. In the model these experiments can be simulated by isotonically changing the sodium activity in the luminal and basolateral baths. The results obtained are given in Fig. 4A together with the experimental results. The reduced model gives already a reasonable fit which can be slightly improved by raising the input value of P^{l}_{Na} up to two orders of magnitude. The response of the model is insensitive to changes in the input value of P^{l}_{Cl} within tree orders of magnitude (above that used in the reduced model) and gives a slightly worse fit to the experimental curve for sodium activities above 10 mM when the input value of P^{bl}_{Na} is increased by two orders of magnitude above that used in the reduced model. The fitting at the higher values of sodium can be improved (not reported here) by adjusting the input value of the affinity of the luminal co-transport system to this ion.

5. Chloride dependence of the equivalent short-circuit current [4]

The chloride dependence of the equivalent short-circuit current was studied experimentally by recording the response of V_{tot} and G_{tot} to the bilateral replacement of Cl^- by an impermeant anion (SO_4^{2-}) and its simulation using the kinetic description and affinities for Na^+, K^+, and Cl^- proposed by Greger [1] is given in Fig. 4B. The curve computed with the reduced model is within the experimental observations but does not fit exactly the smoothed curve published by Greger et al. [4]. The discrepancy, which is not very large at the higher Cl^- activities, increases at the lower values and increases further when the input value of P^{l}_{Na} is increased. The computation is insensitive to changes in the input values of β and P^{l}_{Cl} up to more then two orders of magnitude. A better fit of the model curve is obtained for the lower centrations of Cl^- when the input value of P^{bl}_{Cl} is increased 1000 times. The fitting of the upper values can be improved by adjusting the affinity to Cl^- of the luminal co-transport system (not

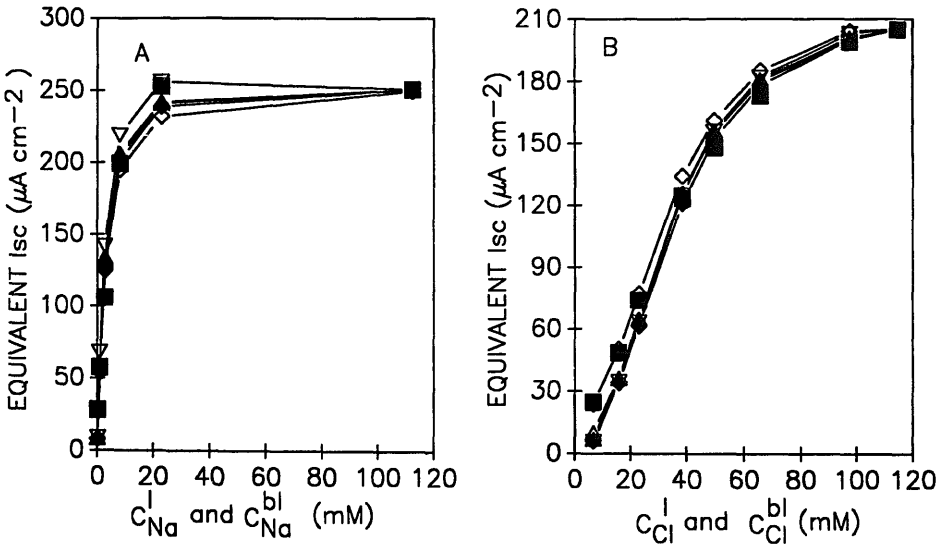

Fig. 4. Kinetics of the chloride and sodium dependence of the equivalent short-circuit current (in $\mu A cm^{-2}$). Na^+ (Panel A) or Cl^- (Panel B) were replaced isotonically by impermeant ions on both sides of the epithelium. Permeability values in $nmcm^{-1}$. Values plotted correspond to published experimental curve (■) and to simulations in which five models were used; reduced (△, see Table I); $P^{l}_{Na} = 10$ (A) or 1 (B) (▽); $P^{l}_{Cl} = 100$ (▲); $P^{bl}_{Na} = 10$ (◇); $\beta = 0.01$ (◆). For meaning of symbols see List of symbols.

reported here). On the whole, the model simulations are in reasonable agreement with the experimental results and the main conclusion to be drawn from them is that the input value of P^{l}_{Na} cannot be more than one order of magnitude larger than that used in the reduced model.

C. Transient responses to inhibitors

A second type of experiment consists of blocking a specialized transport system with a specific inhibitor (ouabain or furosemide). Experimentally the same endogeneous variables as described above were recorded. Assuming that the time-constant of the inhibition of the specific transport system under study is not rate limiting, the speed of the induced changes in V^{l} and V^{bl} and thus in V_{tot} are determined by the turnover of the chamber and by the rates at which the intracellular ion activities change and these rates are determined by the size of the intracellular ion pools and the sizes of the ionic fluxes across the two cellular barriers.

1. The effect of ouabain [10]

The effect of ouabain can be simulated by reducing the maximum rate of pumping $(F_{Max})_p$ through the sodium pump. In the simulations reported below this parameter was made to decay exponentially from its reference value to a value three orders of magnitude smaller with a time-constant of 0.2 s so that after one second the full effect of the drug is obtained. Increasing the time-constant of the decay of $(F_{Max})_p$ will only smooth out the shape of the initial hyperpolarization.

As can be seen from Fig. 5 (left panel) the main difference between the computed curves and the experimental one results from the initial hyperpolarization which is due to the electrogenicity of the pump. Although not seen in the only published experimental curve [10] it was predicted by Greger and Sclatter [2]. This hyperpolarization introduces a delay up to 2 s in the response and is larger, the larger the rate of pumping. As expected, the fall in V_{tot} is speeded up by increasing the input values of P^{bl}_{Na} or P^{l}_{Cl} or P^{l}_{Na} (by 2, 3 and 2 orders of magnitude respectively) in relation to the the corresponding input values of the reduced model and by decreasing the input value of β by two orders of magnitude (which entails and increase in the reference value P^{bl}_{K}), but the curves obtained are still similar to the experimental curve.

2. The effect of furosemide [4]

The effect of furosemide was simulated by reducing exponentially $(F^{l}_{Max})_{cot}$ to 0.001 of its reference value with a time-constant of 0.5 s. In the case of this simulation this time-constant is rate limiting and it was adjusted in such a way that it would fit reasonably both the V^{bl} and the V_{tot} curves. We could not fit exactly both curves because V^{bl} falls faster than V_{tot} and adjusting for one of the curves will worsen the fit for the other. Fig. 5 (right panel) shows that the main discrepancy between the experimental curve and that computed by the reduced model is that in the steady state, after the inhibition has taken effect, the model computes a more negative value of V^{bl} than that observed experimentally. A better fit can be obtained if the input values of P^{l}_{Na} and P^{bl}_{Na} are increased by two orders of magnitude and that of β decreased by 2 orders of

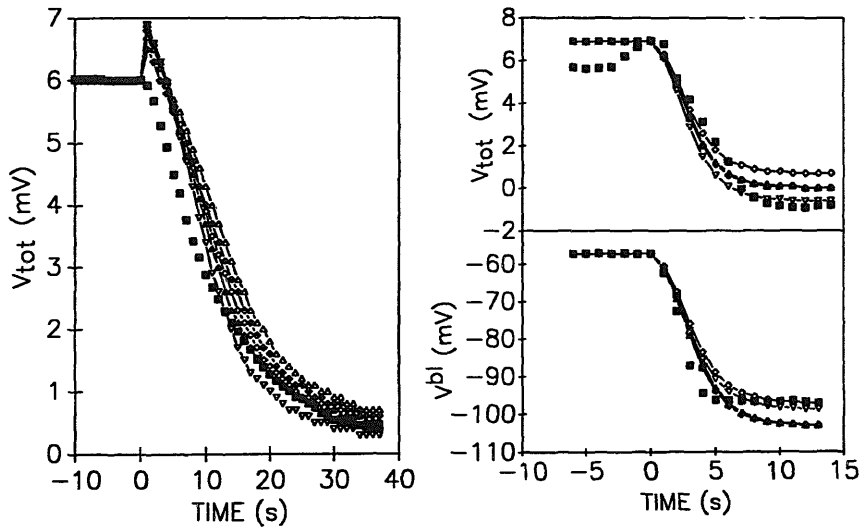

Fig. 5. Time response of V_{tot} to ouabain (left panel) and of V_{tot} and V_{bl} (right panel) to furosemide added at time zero. The effects of ouabain and furosemide were simulated by reducing exponentially (F_{Max}) and $(F^{l}_{Max})_{cot}$ respectively to 0.001 of their reference values. The time constants of the decays were 0.2 and 0.5 s, respectively. Permeability values in nm cm^{-1}. Values plotted correspond to published experimental curve (■) and to simulations in which five models were used; reduced (△, see Table I); $P^{l}_{N1}0$ (△); $P^{l}_{Cl} = 100$ (▽); $P^{bl}_{Na} = 10$ (▲); $\beta = 0.01$ (◇). For meaning of symbols see List of symbols.

magnitude. However, the best fit of the V_{tot} transients are obtained with a P^l_{Na} two orders of magnitude larger than that used in the reduced model.

Discussion

The purpose of this work was to apply mathematical modelling to the cortical thick ascending limb (cTAL) of the rabbit as an attempt to circumvent the limitations of the linear circuit approach in the interpretation of transient electrical phenomena [11,12] as was done with some success in relation to other epithelia [3,12–14]. By providing an integrated description of all the relevant ionic flows across the three epithelial barriers (luminal, basolateral and paracellular), of the time course of intracellular ion activities, of cell volume and of the transmembrane electrical potentials, mathematical modelling of complex systems, such as epithelia, are useful tools in the analysis and the design of experiments since it may reveal relationships which are difficult or impossible to infer intuitively [14].

A large fraction of the data published on the cTAL is suitable for this treatment because it was gathered with the same methodology and also because it is sufficient for the estimation of most of the important parameters of the system. In addition, and as opposed to what happens in relation to volume transporting epithelia (proximal tubule, small intestine, gall bladder), modelling the cTAL, a low resistance salt transporter, does not entail encoding the still controversial mechanisms that have been proposed for isotonic fluid transport. Furthermore, the transport rates of HCO_3^- are very small [15] and there seems to be no evidence that the Na^+/H^+ and Cl^-/OH^- exchange systems play an important role in the experimental conditions under which it was studied [1].

The mathematical model described here is a dynamic extension of the steady state model proposed by Greger and Schlatter [2] and to achieve a concise presentation we describe only those parts of the simulations referring to variables (transmembrane electrical potentials and conductances and equivalent short-circuit current) on which there is data gathered in experiments where the epithelium was challenged with transport inhibitors or changes in the bathing fluids. Even within these constraints we had to reduce the number of simulations reported, since, as explained in Methods, there are four parameters in the system (P^{bl}_{Na}, P^l_{Cl}, P^l_{Na} and β) whose values are not given in the original papers and can not be derived unequivocally from the experimental data. The purpose of this paper is thus to ascertain the simplest version of the model compatible with the published results and not to fully describe its potentialities in making predictions about changes in variables such as volume, flux rates and intracellular ion composition.

In the steady-state linear model proposed by Greger and Schlatter [2] P^{bl}_{Na}, P^l_{Cl} and P^l_{Na} are assumed to be negligible and most of the recirculation of potassium across the basolateral barrier is assumed to take place through a Cl^--K^+ symport. With these assumptions (reduced model) the computed values of G^l and G^{bl} are smaller than the corresponding values indirectly measured reported by Greger[1]. The experimental estimates of the absolute values of G^l and G^{bl} depend very strongly on a precise estimate of the effect of barium on the apical potassium conductance which is not available at the moment and also on a equally precise measurement of VDR. As a result of the uncertainties in both these measurements the main use of our model at this stage is to analyse the sensitivity of G^l and G^{bl} to the different parameters and variables of the system. In all the simulations G^l is almost entirely determined by P^l_K. G^{bl} is also dominated by the chloride conductance of the basolateral barrier. We have shown that G^l is very sensitive, within certain ranges, to the input values (for the reference state) of C^c_K, I^c and that G^{bl} is sensitive to C^l_{Cl}, β and I^c. Adjustment of the intracellular potential is of limited use since it affects G^l and G^{bl}in opposite directions. This means that an appropriate choice of the values of those input quantities, in particular of I^c will lead do a better fit of the reference state in relation to G^{bl} and G^l. Both these conductances are very sensitive to P^l_{Na} because an increase in the permeability of the luminal membrane to sodium while maintaining I^c fixed entails also a much larger flux across the luminal Na-K-2Cl symport, a larger backflux of potassium across this membrane, hence a higher P^l_K and also a larger diffusional outflux of potassium across the basolateral barrier (higher P^{bl}_K) to compensate for a higher rate of pumping. The same is observed but to a lesser degree if the equivalent short-circuit current is fixed. However, as shown by other simulations (see Fig.3) the input value of P^l_{Na} cannot be increased much above 1 $nm\,cm^{-1}$. The input value of P^l_{Cl} also influences G^l but increasing its value to 100 $nm\,cm^{-1}$ will worsen the fitting of the simulations of the dilution potentials. Neither of the conductances is sensitive to P^{bl}_{Na} in the range of 0.1 to 100 $nm\,cm^{-1}$.

In another group of simulations (Tables II and III) only values at steady state before and after the perturbation are presented. One should not expect an exact fit with these simulations since values of G_{tot} are not given for most of the experiments in the original papers. For the experiments in which step changes in the activities of potassium or chloride in luminal fluid or a reduction of P^l_K (effect of barium) were induced, using higher values of P^l_{Cl} and P^l_{Na} than those used in the reduced model led to an overall best fit. The simulations of similar step changes performed on the basolateral side are difficult to analyse as a result of the larger scatter in the experimental results. At most we can say that the computed values fall within the range of the

experimental values. The simulations of the effect of barium applied to the basolateral side show, as predictable, that the largest changes in VDR are obtained when β is small (0.01) but the difference between the two models (high and low β) is very small for low input values of P_{Na}^{bl}. This is because for low input values of P_{Na}^{bl}, most of G^{bl} is due to the chloride conductance of the basolateral barrier. Overall our simulations support the model proposed by Greger and co-workers but they also show that the differences between the two alternative models tested here (with or without a dominant K-Cl cotransport in the basolateral barrier) are not sufficiently marked to justify a clear cut choice based on the barium experiments.

The least satisfactory simulations were those referring to the NaCl dilution potentials. Greger [9] observed a symmetrical response of V_{tot}. The reduced version of our model gave a good fit when the effect of reducing the NaCl activity on the luminal side was simulated and could be improved by increasing the shunt conductance through the choice of a lower input value of V_{tot}. The computed response by the reduced model to changes in NaCl activity on the basolateral side was much smaller than that observed experimentally because P_{Cl}^{bl} is very similar to P_{Na}^{sh}. A better fit is obtained by increasing the shunt conductance as discussed above or by increasing P_{Na}^{bl} but this permeability, as shown in the other simulations has an upper limit of 10 nm s^{-1}.

The simulations of the dependence of the equivalent short-circuit current on sodium or chloride give a reasonable fit to the experimental curves except at the very low activities of both sodium or chloride at which, experimentally there is an unexplained residual current. Both curves are insensitive to a decrease in the input value of β up to two orders of magnitude, of P_{Cl}^{bl} up to three orders of magnitude and of P_{Na}^{l} up to two orders of magnitude. The upper limit of P_{Na}^{bl} still compatible with a good fitting to both curves was 1 nm s^{-1}.

The transient behaviour of the model was analyzed in relation to the effect of furosemide and ouabain.

If the effect of furosemide is simulated by reducing instantaneously $(F_{Max}^{l})_{cot}$ to a negligible fraction (0.001) of the reference value, both V_{tot} and V^{bl} fall much faster than observed experimentally. This suggests either a slow binding to the transport system or, more likely, that the turnover of the perfusion system is rate limiting. We adjusted the speed of the computed response by adjusting the time-constant of the decay of $(F_{Max}^{l})_{cot}$. For the experiment that was simulated the best fit was obtained with a P_{Na}^{l} of 10 nm s^{-1} but reasonable fits were obtained for all the reference states tested and in the absence of more experimental data we cannot make a final choice.

To simulate the effect of ouabain, $(F_{Max})_p$ was made to decay exponentially with a time-constant of 0.2 s. The computed time course of the decay V_{tot} was much slower than in the case of the furosemide inhibition and was affected by the speed at which $(F_{Max})_p$ decayed only for time-constants larger than 1 s. The main difference between the simulations and the experimental curves was the initial hyperpolarization computed by the model, an effect not observed in the only published experimental curve, but originally predicted by Greger and Schlatter[2]. Both the reduced model and the the other five versions of the model (see Fig. 5) gave very similar results. The hyperpolarization might be easily missed experimentally because it is quite small (less than 1 mV) and it will be smoothed out should the time-constant of the ouabain action be larger than that used in the simulations, in which case there will be only a delay in the effect.

The overall conclusion to be drawn from this work is that even in its simplest (reduced) version, which corresponds to the model originally proposed by Greger and co-workers based on linear circuit analysis, our model reproduces closely most of the published experimental results. In the cases in which the fit was less satisfactory it still provides a useful tool which can be used to identify possible causes for the discrepancies.

A further development of the model is to extend it in order to encompass a tubular geometry of the epithelium and more physiological conditions in which the flow of fluid along the luminal and basolateral membranes becomes rate limiting.

List of symbols

$(A^{bl})_{cot}$	Phenomenological constant relating the intracellular and basolateral concentrations of K and Cl with the flux of KCl $(F^{bl})_{cot}$ through the K-Cl cotransport located in the basolateral barrier (mol^{-1}cm^4 s^{-1}).
β	Fraction of the potassium flux through the Na/K pump that recirculates through the basolateral K-Cl symport.
C_K^{bl}	Activity of K in the basolateral bath (mol cm^{-3}).
C_{An}^{c}	Intracellular activity of non-diffusible anions of valence n (mol cm^{-3}).
C_{Cl}^{c}	Intracellular activity of Cl (mol cm^{-3}).
C_K^{c}	Intracellular activity of K (mol cm^{-3}).
C_{Na}^{c}	Intracellular activity of Na (mol cm^{-3}).
C_{iso}	Osmolarity of external baths (mol cm^{-3}).
C_{Cl}^{l}	Activity of Cl in the luminal bath (mol cm^{-3}).
C_K^{l}	Activity of K in the luminal bath (mol cm^{-3}).
C_{Na}^{l}	Activity of Na in the luminal bath (mol cm^{-3}).
cTAL	Cortical thick ascending limb.
E	Dimensionless quantity defined as $Z_i \cdot F \cdot V/R \cdot T$.
F	Faraday's constant (96 500 coul equiv.$^{-1}$).

F_{Cl}^{bl} Flux of chloride across the basolateral barrier ($mol\,cm^{-2}\,s^{-1}$).

$(F_{Cl}^{l})_{cot}$ Flux of chloride through the luminal cotransport ($mol\,cm^{-2}\,s^{-1}$).

F_{Cl}^{l} Flux of chloride across the luminal barrier ($mol\,cm^{-2}\,s^{-1}$).

$(F^{bl})_{cot}$ Flux of KCl through the basolateral cotransport ($mol\,cm^{-2}\,s^{-1}$).

$(F^{l})_{cot}$ Flux of Na or K or 0.5 of the Cl flux through the Na + K + 2Cl luminal cotransport ($mol\,cm^{-2}\,s^{-1}$).

F_{K}^{bl} Flux of potassium across the basolateral barrier ($mol\,cm^{-2}\,s^{-1}$).

$(F_{K}^{l})_{cot}$ Flux of potassium through the luminal cotransport ($mol\,cm^{-2}\,s^{-1}$).

F_{K}^{l} Flux of potassium across the luminal barrier ($mol\,cm^{-2}\,s^{-1}$).

$(F_{K})_{p}$ Flux of potassium through the sodium pump ($mol\,cm^{-2}\,s^{-1}$).

$(F_{Max})_{cot}$ Maximum rate of transport through the luminal cotransport ($mol\,cm^{-2}\,s^{-1}$).

F_{Na}^{bl} Flux of sodium across basolateral barrier ($mol\,cm^{-2}\,s^{-1}$).

$(F_{Na}^{l})_{cot}$ Flux of sodium through the luminal cotransport ($mol\,cm^{-2}\,s^{-1}$).

F_{Na}^{l} Flux of sodium across the luminal barrier ($mol\,cm^{-2}\,s^{-1}$).

$(F_{Na})_{p}$ Flux of sodium through the sodium pump ($mol\,cm^{-2}\,s^{-1}$).

$(F_{Max})_{p}$ Maximum rate of pumping by the sodium pump ($mol\,cm^{-2}\,s^{-1}$).

G^{bl} Conductance of basolateral barrier ($S\,cm^{-2}$).

G^{l} Conductance of luminal barrier ($S\,cm^{-2}$).

G_{tot} Total trans-epithelial conductance ($S\,cm^{-2}$).

I^{bl} Total ionic current density across basolateral barrier ($A\,cm^{-2}$).

I^{c} Total ionic current density across the cellular pathway ($A\,cm^{-2}$).

I_{i} Total ionic current density due to the flow of ion i ($A\,cm^{-2}$).

I^{l} Total ionic current density across luminal barrier ($A\,cm^{-2}$).

I_{sc} Equivalent short circuit current ($A\,cm^{-2}$), computed as the product $G_{tot} \cdot V_{tot}$.

I^{sh} Total ionic current density through the paracellular pathway ($A\,cm^{-2}$).

I_{tot} Total trans-epitheial current density ($A\,cm^{-2}$).

$(K_{Cl})_{cot}$ Affinity for chloride of luminal Na-K-2Cl cotransport ($mol\,cm^{-3}$).

$(K_{i})_{cot}$ Affinity for ion i of luminal Na-K-2Cl cotransport ($mol\,cm^{-3}$).

K_{K} Apparent affinity of the sodium pump for basolateral potassium ($mol\,cm^{-3}$).

$(K_{K})_{cot}$ Affinity of the Na-K-2Cl cotransport for potassium ($mol\,cm^{-3}$).

K_{Na} Apparent affinity of the sodium pump for intracellular sodium ($mol\,cm^{-3}$).

$(K_{Na})_{cot}$ Affinity of the Na-K-2Cl cotransport for sodium ($mol\,cm^{-3}$).

n Valence of impermeant intracellular anions ($equiv.\,mol^{-1}$).

P_{Cl}^{bl} Permeability of basolateral barrier to chloride ($cm\,s^{-1}$).

P_{K}^{bl} Permeability of basolateral barrier to potassium ($cm\,s^{-1}$).

P_{Na}^{bl} Permeability of basolateral barrier to sodium ($cm\,s^{-1}$).

P_{Cl}^{l} Permeability of luminal barrier to chloride ($cm\,s^{-1}$).

P_{K}^{l} Permeability of luminal barrier to potassium ($cm\,s^{-1}$).

P_{Na}^{l} Permeability of luminal barrier to sodium ($cm\,s^{-1}$).

P_{Cl}^{sh} Permeability of paracellular pathway to chloride ($cm\,s^{-1}$).

P_{K}^{sh} Permeability of paracellular pathway to potassium ($cm\,s^{-1}$).

P_{Na}^{sh} Permeability of paracellular pathway to sodium ($cm\,s^{-1}$).

Q_{Na} Total intracellular amount of sodium ($mol\,cm^{-2}$).

Q_{K} Total intracellular amount of potassium ($mol\,cm^{-2}$).

Q_{Cl} Total intracellular amount of chloride ($mol\,cm^{-2}$).

R Molar gas constant ($8.315\ J\,deg^{-1}\,mol^{-1}$).

T Absolute temperature (K).

V Voltage (volt)

V^{bl} Electrical potential difference across basolateral barrier (volt).

VDR Voltage divider ratio, calculated as G^{bl}/G^{l}.

V^{l} Electrical potential difference across luminal barrier (volt).

V_{tot} Trans-epithelial electrical potential difference (volt).

Z_{i} Valence of ion i ($equiv.\,mol^{-1}$)

The dimensions given in the above list of symbols are those used in the computations. For convenience, in the tables and figures the following units will be used: voltages, mV; activities and affinities, mM; currents, $\mu A\,cm^{-2}$; conductances, $mS\,cm^{-2}$; permeabilities, $nm\,s^{-1}$.

References

1 Greger, R. (1985) Physiol. Rev. 65, 760–797.

2 Greger, R. and Schlatter, E. (1983) Pflügers Arch. 396, 325–334.

3 Lew, V.L., Ferreira, H.G. and Moura, T. (1979) Proc. R. Soc. Ser. B 206, 53–83.

4 Greger, R., Schlatter, E. and Lang, F. (1983) Pflügers Arch. 396, 308–314.
5 Hodgkin, A.L. and Katz, B. (1949) J. Physiol. (Lond.) 108, 37–77.
6 Neal, F. and Shone, R. (1976) Economical Model Building, Macmillan Press, London.
7 Baerentsen, H., Giraldez, F. and Zeuthen, T. (1983) J. Membr. Biol. 75, 215–218.
8 Greger, R. and Schlatter, E. (1983) Pflügers Arch. 396, 315–324.
9 Greger, R. (1981) Pflügers Arch. 390, 30–37.
10 Greger, R. and Fromter, E. (1980) in Adv. Physiol. Sci., Vol. 11, Kidney and Body Fluids (Takacs, L., ed.), pp. 375–379, Pergamon Press, Budapest.
11 Finkelstein, A. and Mauro, A. (1963) Biophys. J. 3, 215–237.
12 Civan, M.M. and Bookman, R.J. (1982) J. Membr. Biol. 65, 63–80.
13 Lindemann, B. (1977) Bioelectrochem. Bioenerg. 4, 275–286.
14 Larsen, E.H. and Rasmussen, B.E. (1982) Philos. Trans. R. Soc. Ser. B 299, 413–434.
15 Hno, Y. and Burg, M.B. (1981) Jap. J. Physiol. 31, 99–107.